Nanopores in carbon nitride nanotubes: Reversible hydrogen storage sites

Se Yun Kim, Hyun Seok Kim, Saji Augustine, and Jeung Ku Kang

Citation: Appl. Phys. Lett. **89**, 253119 (2006); doi: 10.1063/1.2422912
View online: http://dx.doi.org/10.1063/1.2422912
View Table of Contents: http://apl.aip.org/resource/1/APPLAB/v89/i25
Published by the American Institute of Physics.

Nanopores in carbon nitride nanotubes: Reversible hydrogen storage sites

Se Yun Kim, Hyun Seok Kim, Saji Augustine, and Jeung Ku Kang[a)]
Department of Materials Science and Engineering, Korea Advanced Institute of Science and Technology, Daejeon 305-701, Republic of Korea

(Received 21 September 2006; accepted 22 November 2006; published online 22 December 2006)

Experimental and theoretical approaches are used to determine hydrogen storage mechanisms in nanopores of multiwalled carbon nitride nanotubes (MWCNNTs). First, the authors produce ~0.6 nm pores on the stems of MWCNNTs by plasma-enhanced chemical vapor deposition. Next, thermal desorption spectra were measured and obtained two different peaks. This is explained by hydrogen desorption barriers of 0.36–0.50 eV attributed to two different types of ~0.6 nm pores. Moreover, H_2 adsorption between complete interlayers is found to be endothermic by 1.27 eV. In this respect, open channels and ~0.6 nm pores on MWCNNTs are considered to provide the route for reversible hydrogen storage. © *2006 American Institute of Physics*. [DOI: 10.1063/1.2422912]

Hydrogen is an attractive fuel alternative to conventional hydrocarbon fuels because water is the only product when hydrogen burns with oxygen in a fuel cell. On the other hand, one of the main issues for hydrogen economy is the development of a suitable hydrogen storage material that is small, light, and safe. In addition, achieving at least the weight percent of 6.5 wt % is the goal of the U.S. Department of Energy. Because of these requirements, early in the development of hydrogen storage materials various carbon materials were investigated.[1] This is because carbon materials can give many different types of structures, which provide a variety of hydrogen storage sites. For example, the carbon nanotubes (CNTs) having high surface-to-volume ratios were suggested as ideal structures for fast kinetics because of their reversible characteristics during hydrogenation and dehydrogenation.

Despite these advantages, recent studies[2,3] have shown that the hydrogen stored on a pristine CNT is less than 0.01 wt % at 1 bar condition and room temperature. Moreover, the recent experiment by Lawrence and Xu[4] confirmed that only 0.6 wt % hydrogen at room temperature was adsorbed on the CNT bundle at the high pressure condition of 100 bars. Also our recent study[5] showed that liquefaction of H_2 molecules on the CNT bundle still occurs at the low temperature of about 80 K under the pressure conditions larger than 20 bars. In this respect, to use pristine CNTs as hydrogen storage media could be impractical for practical applications at atmospheric conditions due to the expensive cryogenic process for hydrogen adsorption (80–150 K at 1 bar) on the CNT surfaces.

On the other hand, here we find that nanopores with ~6 Å diameters on the stems of the nanotubes are capable of giving great potentials to reversible hydrogen storage sites. This is because the physical interaction distance between the H_2 molecule and C atom of a carbon-based nanotube is ~3 Å. In this respect, the minimum diameters of nanopores for possible penetration of H_2 should be twice of ~3 Å (= ~6 Å). However, if carbon atoms bonded in the perimeter of carbon-based nanopores could be replaced with other elements such as nitrogen atoms (or hereafter called as the carbon nitride nanotube or CN_x), the physical interaction diameters of N-doped nanopores for possible penetration of H_2 could be reduced such that hydrogen could desorb at the temperatures ranging from room temperature to 80 °C, which is the ideal condition for various applications. Here, we report that the carbon nitride nanotube having 6 Å pores is an ideal structure being capable of satisfying the required temperature condition. Our experiments also demonstrate that versatile 6 Å pores could be created on the stems of the multiwalled carbon nitride nanotubes with the uniform distribution, as shown in Fig. 1.

Carbon nitride nanotubes were synthesized using a microwave plasma-enhanced CVD (PECVD). First, a 7-nm-thick Co layer was deposited on a SiO_2/Si substrate via rf sputtering with 100 W rf power. The thickness of SiO_2 on the Si wafer was 500 nm. Then, the substrate was moved

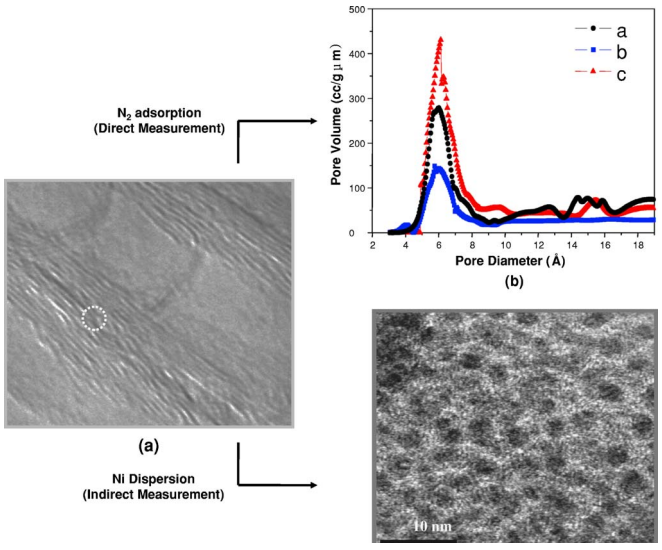

FIG. 1. (Color online) (a) High-resolution transmission electron microscope (HRTEM) image of a carbon nitride nanotube (CN_x, x=0.008), where the white circle represents the disconnected graphene layers corresponding to the nanopores. (b) The Horvath-Kawazoe pore size distribution obtained from the carbon nitride nanotubes grown with "a" (15 SCCM of CH_4 and 85 SCCM of N_2), "b" (15 SCCM of CH_4, 55 SCCM of N_2, and 30 SCCM of H_2), and "c" (15 SCCM of CH_4, 81 SCCM of N_2, and 4 SCCM of O_2), and (c) HRTEM image of carbon nitride nanotubes with dispersed Ni nanoparticles.

[a)]Author to whom correspondence should be addressed; FAX: +82-42-869-3310; electronic mail: jeungku@kaist.ac.kr

to the PECVD chamber and the chamber was evacuated to about 0.1 Torr. Next, the substrate was heated to 720 °C in a vacuum by a halogen lamp. After that, the N_2 gas was flowed into the chamber and the substrate was treated by the N_2 plasma created using a microwave power of 750 W for 1 min. Then, 15 SCCM (SCCM denotes cubic centimeter per minute at STP) of CH_4 was introduced at 850 °C, either with N_2 only or with N_2 and H_2 gases simultaneously, and the microwave power was increased to 800 W. Different flow rates of N_2, H_2, and O_2 gases were used in each experiment. The growth time was 20 min. The morphology and the structure of the as-grown samples were analyzed via high-resolution transmission electron microscopy (HRTEM) (FE-TEM F20, Phillips). The pore distribution of the grown nanotubes was analyzed as received from the isotherm of the N_2 adsorption on the samples (Autosorb-3B, Quantachrome). Also for direct observation of nanopores created on the stems of the nanotubes, Ni nanoparticles were dispersed on their stems by the method described in the previous work.[6] In addition, the gas chromatograph equipped with the thermal conductivity detection method and the selected capillary column (Carboxen 1006PLOT) are used to observe the hydrogen desorption property.

Figure 1(a) shows the HRTEM image of a carbon nitride nanotube where the disconnected graphene layers (in a circle) represent nanopores, while Fig. 1(b) compares the pore size distribution of the as-grown nanotubes with respect to different flow rates of N_2, H_2, and O_2 gases. The ~6 Å pores are shown on all the grown nanotubes. The volume of ~6 Å pores increased for the samples grown with an increased nitrogen flowing rate, with the minimum volume observed for those nanotubes grown at 30 SCCM of hydrogen, 55 SCCM of nitrogen, and 15 SCCM of methane. In addition the peak around 16 Å disappeared after an inclusion of 30 SCCM of H_2 during growth. On the other hand, nanotubes grown with 4 SCCM of oxygen had the largest volume of ~6 Å pores, which was about three times larger than that of nanotubes grown with 30 SCCM of H_2, 55 SCCM of nitrogen, and 15 SCCM of CH_4. Figure 1(c) shows that Ni nanoparticles can be uniformly dispersed, implying that nanopores were uniformly created on our synthesized nanotubes.

To determine the origin of the different volumes of nanopores, x-ray photon spectroscopy (XPS) analyses were performed. We were confirmed that our samples were carbon nitride nanotubes from the N 1*s* signal of the XPS spectrum of the as-grown sample, as shown in Fig. 2. The N 1*s* XPS spectra were divided by three Lorentz fits: (a) 398.2 eV is the tetrahedral nitrogen phase (N1) bonded to an sp^3-hybridized carbon, (b) 401.3 eV is the trigonal nitrogen phase (N2) bonded to an sp^2-coordinated carbon, and (c) 404.8 eV is the molecular N_2, where the binding energy of 404.8 eV is lower than original binding energy of free N_2 gas of 409.9 eV because of the screening effect between N 1*s* core hole and matrix. The molecular N_2 may be attributed to the trapped N_2 gas in the holes between the nodes in the CN_x nanotubes. The ratio of peak intensities of the N1 or N2 ($I_{Ni}/I_{N1}+I_{N2}$) was examined. The relative peak intensity, 0.378, for tetrahedral nitrogen atoms bonded to an sp^3-hybridized carbon ($I_{N1}/I_{N1}+I_{N2}$) of CN_x nanotubes grown with only N_2 and CH_4 is stronger than the 0.306 for nanotubes grown with N_2, H_2, and CH_4. In addition, the more N contents the nanotubes have, the poorer the crystallinity they have. On the other hand, in contrast with carbon nanotubes, the CN_x nanotubes have open edges of graphene layers on the nanotube stems. The open edges of graphene layers are considered to be caused by N substitution for C atoms on the stems of CN_x nanotubes. The intensities of the binding energies at 404.8 eV are different from the nanotubes with different growing gases. The nanotubes with 15 SCCM CH_4 and 85 SCCM N_2 have the strongest intensity from among the three samples. Moreover, the nanotubes with 15 SCCM CH_4, 55 SCCM of N_2, and 30 SCCM of H_2 have the lowest molecular N_2 binding energy peak. This result indicates that the amount of N_2 during nanotubes' growth has an important effect on the structure of as-grown nanotubes. Interestingly, the nanotubes having the largest volume of ~6 Å pores were those grown with 4 SCCM of O_2. The relative intensity of the N1 peak ($I_{N1}/I_{N1}+I_{N2}$) of the nanotubes grown with 4 SCCM of O_2 is 0.448, which is the highest, indicating that these nanotubes have the poorest crystallinity among the grown nanotubes. Therefore, the N 1*s* XPS spectra can explain the different volumes of pores created on the samples.

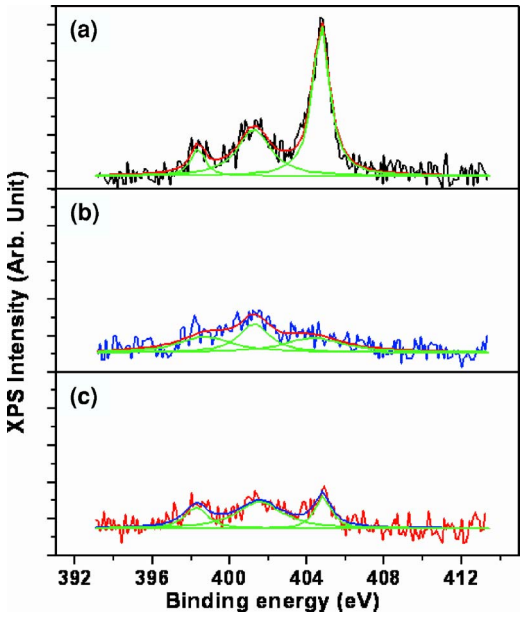

FIG. 2. (Color online) N 1*s* XPS spectra of the carbon nitride nanotubes grown with (a) 15 SCCM of CH_4 and 85 SCCM of N_2; (b) 15 SCCM of CH_4, 55 SCCM of N_2, and 30 SCCM of H_2; and (c) 15 SCCM of CH_4, 81 SCCM of N_2, and 4 SCCM of O_2.

We used both the experiment using thermal desorption spectra and the first-principles calculation method, as summarized in Fig. 3, to determine hydrogen-ensnaring mechanism in nanopores with ~0.6 nm sizes of carbon nitride nanotubes. The top and side models used for simulation for ~0.6 nm N-doped nanopores are shown in Fig. 3(a), where N-doped (or undoped) nanopores are made of alternating N (or C) and C atoms after one benzene ring unit has been removed from the carbon graphene layer. We use the PW91 (Ref. 7) method in the CASTEP (Ref. 8) program to investigate hydrogen storage and desorption mechanisms on about 6 Å pores created in the stems of double-walled nanotubes with periodic boundary conditions, where all atoms are described using nonlocal norm-conserving Vanderbilt scalar pseudopotentials.[9] The set of *k* points used to expand the molecular wave function is based on the Monkhorst-Pack

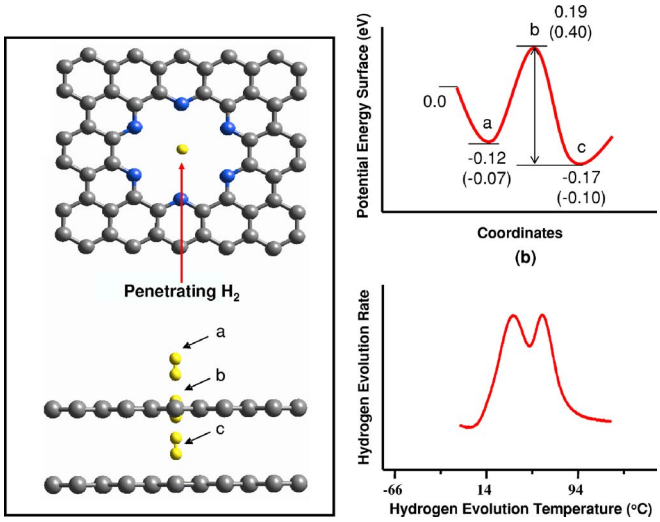

FIG. 3. (Color online) (a) Top and side views of penetration H_2 through N-doped nanopores and (b) the potential energy surface of hydrogen ensnared in the nanopores of multiwalled carbon nitride and carbon nanotubes, where the values in parentheses represent the energies on micropores with only carbon atoms on their edges, where a is the adsorption site for H_2 on the exterior wall, b is the transition state site for penetration of H_2 through the pore, and c is the adsorption site for H_2 ensnared between the neighboring pores. (c) The H_2 thermal desorption spectra obtained from the nanotubes with ~40 nm diameters. Gray, blue, and yellow colors represent C, N, and H atoms, respectively.

scheme.[10] We use a plane-wave basis that is truncated to include plane waves having kinetic energies of less than 240 eV. There are four configuration for H_2 on Fig. 3(a): (1) free H_2, (2) H_2 physisorption on the exterior wall denoted as "a" in Fig. 3(a), (3) H_2 penetration through the nanopore denoted as "b" in Fig. 3(a), and (4) H_2 physisorption between the two nanopores denoted as "c" in Fig. 3(a). The physisorption energy of a hydrogen molecule on the outside of nanopores in a doubled-walled carbon nitride nanotube was −0.12 eV [see Fig. 3(b)], which is different from the −0.07 eV of a double-walled carbon nanotube. The distance between the center of the adsorbing hydrogen molecule and the nanotube surface was 2 Å. In addition, the activation barrier for hydrogen penetration through the nanopore from the outside to the inside of the nanotube at b in Figs. 3(a) and 3(b) was 0.31 eV. This barrier is found to be much lower than that for the single-wall carbon nanotube (SWNT). Indeed, Ma *et al.*[11] estimated that hydrogen molecules need at least ~16.5 eV to pass through a hexagon ring of SWNT. Also the penetration barrier of 0.31 eV is lower than the barrier of 0.47 eV for H_2 penetration through ~0.6 nm pores in a multiwalled carbon nanotube. Hydrogen molecules adsorbed between two nanopores are more stable than the free hydrogen molecules by 0.17 eV, which is compared to the 0.10 eV on a pure MWCNT. Consequently, 0.36–0.50 eV [see Fig. 3(b)] are required to discharge the hydrogen molecules adsorbed between the walls of carbon nitride nanotubes, which appears to be consistent with our experimental hydrogen thermal desorption spectra, as obtained in Fig. 3(c). In this respect, it is considered that ~0.6 nm size pores created on the stems of carbon nitride nanotubes may consist of two different types: the first case is that their carbon atoms on the pore edges are fully replaced by nitrogen atoms while in the other case they just include carbon atoms. In addition, hydrogen ensnared between interlayers with complete benzene ring units (that is with no pore) is found to be unstable due to its having endothermic adsorption energy of 1.27 eV, implying that many interlayers existing inside MWCNNTs could reduce hydrogen storage capacity compared to the double-walled nanotube structures. In this respect, versatile 0.6 nm pores on the stems of double-walled carbon nitride nanotubes are here proposed to be ideal structures for reversible hydrogen storage. For example, the ~0.6 nm nanopore sites constructed by one benzene ring unit missing can be used to store hydrogen. In addition open channels with two benzene rings missing, connecting directly the outside with the inside of the double-walled nanotubes, could be used to store hydrogen inside the wall of the nanotube. The storage method through open channels is capable of giving the increasing hydrogen storage capacities larger than 7 wt % hydrogen as the pressures increase to the moderate values, attributed to many free spaces made by bamboolike structures of carbon nitride nanotubes [see Fig. 1(a)].

In conclusion, hydrogen ensnared in about 6 Å sized nanopores of a multiwalled carbon nitride nanotubes are found to be capable of being released at two different temperature ranges as they have the desorption barriers of 0.36 and 0.50 eV, but hydrogen insertion into the complete interlayer space of a multiwalled carbon nitride nanotube is determined to be endothermic by 1.27 eV. Consequently, these results imply that versatile open channels and ~0.6 nm pores created on MWCNNTs could provide the proper route to reversible hydrogen storage media usable for practical applications.

This work was supported by Grant No. M103KW010017-06K2301-01720 from the Hydrogen Energy R & D program of the Ministry of Science and Technology.

[1] A. C. Dillon and M. Heben, Appl. Phys. A: Mater. Sci. Process. **72**, 133 (2001).
[2] S. S. Han and H. M. Lee, Carbon **42**, 2169 (2004).
[3] A. Ansón, M. A. Callejas, A. M. Benito, W. K. Maser, M. T. Izquierdo, B. Rubio, J. Jagiello, M. hommes, J. B. Arra, and M. T. Martínez, Carbon **42**, 1243 (2004).
[4] J. Lawrence and G. Xu, Appl. Phys. Lett. **84**, 918 (2004).
[5] S. S. Han, J. K. Kang, and H. M. Lee, Appl. Phys. Lett. **86**, 203108 (2005).
[6] H. S. Kim, H. Lee, H. K. S. Han, J. H. Kim, M. S. Song, M. S. Park, J. Y. Lee, and J. K. Kang, J. Phys. Chem. B **109**, 8983 (2005).
[7] J. P. Perdew and Y. Wang, Phys. Rev. B **45**, 13244 (1992).
[8] M. C. Payne, M. P. Teter, D. C. Allan, T. A. Arias, and J. D. Joannopoulos, Rev. Mod. Phys. **64**, 1045 (1992).
[9] D. Vanderbilt, Phys. Rev. B **41**, 7892 (1990).
[10] H. J. Monkhorst and J. D. Pack, Phys. Rev. B **13**, 5188 (1976).
[11] (10) Y. Ma, Y. Xia, M. Zhao, M. Ying, X. Liu, and P. Liu, J. Chem. Phys. **115**, 8152 (2001).